Temperature Dependence of Fusion Kinetics and Fusion Pores in Ca^{2+}-triggered Exocytosis from PC12 Cells

Zhen Zhang and Meyer B. Jackson

Department of Physiology and Molecular and Cellular Pharmacology Ph.D. Program, University of Wisconsin School of Medicine and Public Health, Madison, WI 53706

The temperature dependence of Ca^{2+}-triggered exocytosis was studied using carbon fiber amperometry to record the release of norepinephrine from PC12 cells. Single-vesicle fusion events were examined at temperatures varying from 12 to 28°C, and with release elicited by depolarization. Measurements were made of the initial and maximum frequencies of exocytotic events, of fusion pore lifetime, flux through the open fusion pore, kiss-and-run versus full-fusion probability, and parameters associated with the shapes of amperometric spikes. The fusion pore open-state flux, and all parameters associated with spike shape, including area, rise time, and decay time, had weak temperature dependences and activation energies in the range expected for bulk diffusion in an aqueous solution. Kiss-and-run events also varied with temperature, with lower temperatures increasing the relative probability of kiss-and-run events by ~50%. By contrast, kinetic parameters relating to the frequency of exocytotic events and fusion pore transitions depended much more strongly on temperature, suggesting that these processes entail structural rearrangements of proteins or lipids or both. The weak temperature dependence of spike shape suggests that after the fusion pore has started to expand, structural transitions of membrane components are no longer kinetically limiting. This indicates that the content of a vesicle is expelled completely after fusion pore expansion.

INTRODUCTION

The efficacy of synaptic transmission depends strongly on temperature and this often reflects a strong temperature dependence of exocytosis (Takeuchi, 1958; Katz and Miledi, 1965; Weight and Erulkar, 1976; Sabatini and Regehr, 1996; Volgushev et al., 2004). To investigate the temperature dependence of exocytosis, we have investigated norepinephrine release from PC12 cells, where voltammetry measurements have shown that exocytosis has a similar strong temperature dependence (Earles et al., 2001). We have used carbon fiber amperometry recording, which detects Ca^{2+}-triggered exocytosis from single vesicles, and thus provides a means of studying the temperature dependence of exocytosis in greater detail. Amperometric recording of the release of biogenic amines from cells has contributed a great deal to our understanding of Ca^{2+}-triggered exocytosis. Using carbon fiber microelectrodes, amperometry can detect the fusion of a single vesicle (Wightman et al., 1991) and resolve single-vesicle fusion events into a temporal sequence of distinct steps (Chow et al., 1992; Jankowski et al., 1993; Zhou et al., 1996; Ales et al., 1999; Wang et al., 2001). This temporal sequence contains a wealth of information about the kinetic mechanism of vesicle fusion.

The first detectable feature revealed in an amperometric recording of vesicle fusion is the foot signal. This slow trickling of norepinephrine through an initial fusion pore signals the first aqueous contact between the vesicle lumen and extracellular volume. After a fusion pore opens, the amperometric current remains low until the fusion pore either closes or starts to expand. When expansion starts, the amperometric current then rises sharply to generate a spike of catecholamine flux as the rate of expulsion of vesicle content accelerates dramatically. This characteristic sequence in the single-vesicle release waveform (foot→spike) reports membrane transitions from closed fusion pores to open fusion pores to dilating fusion pores. Quantitative analysis of these transitions can provide insight into the kinetic mechanism of exocytosis.

During these steps of exocytosis, norepinephrine escapes from a vesicle and then diffuses through the bulk extracellular fluid to the carbon fiber electrode. Depending on the size of the open fusion pore, either the first or second process can limit the flux of catecholamine. A fusion pore could be sufficiently narrow so that its size limits catecholamine flux, and in that situation the amperometric signal can provide information about the structure and dynamics of the fusion pore (Spruce et al., 1990; Jackson, 2007). However, when the fusion pore is large, its size becomes irrelevant. In this case the rate of catecholamine loss from a vesicle can reflect either release from a protein matrix inside a vesicle or diffusion through bulk solution to the carbon fiber electrode (Wightman et al., 1995). Diffusion generally has a weak temperature

Correspondence to Meyer Jackson: mjackson@physiology.wisc.edu

Abbreviation used in this paper: RMS, root-mean-square.

J. Gen. Physiol. © The Rockefeller University Press $30.00
Volume 131 Number 2 February 2008 117–124
http://www.jgp.org/cgi/doi/10.1085/jgp.200709891

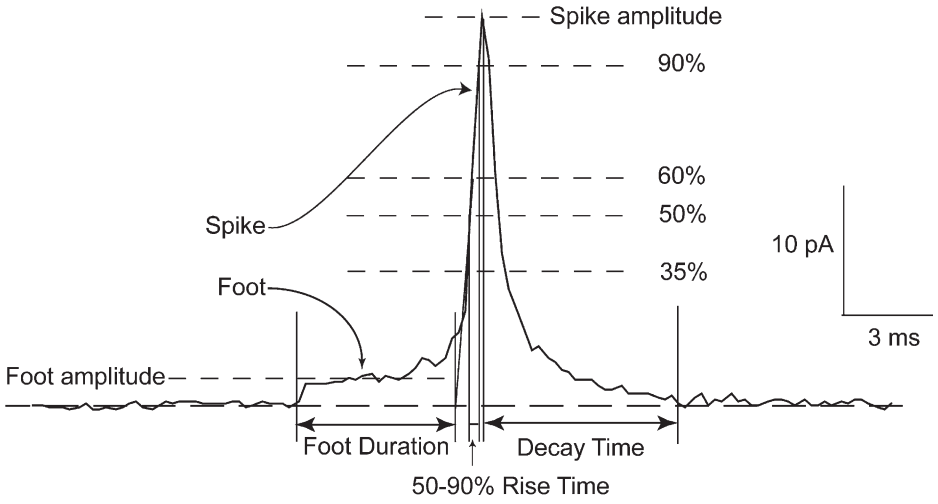

Figure 1. An amperometry recording of the fusion of a single vesicle. The foot reports the opening of a fusion pore and the spike begins when the fusion pore enters into an expansion phase. The features of feet and spikes analyzed in this study are illustrated. We measured the amplitude and duration of the foot, the peak amplitude, total area, width at half-height, time to rise from 35 to 90% of peak, and time to decay from 90% to within 5×RMS of baseline. The method of computing these various parameters is described in Materials and methods.

dependence that follows the relatively low temperature dependence of diffusion constants of solutes in water (Robinson and Stokes, 1965). However, some of the steps of exocytosis depend on complex rearrangements of proteins and lipids. These processes should have large activation energies and hence very steep temperature dependences. To evaluate the relative roles of diffusion and protein/lipid rearrangements as the fusion of a vesicle progresses through successive stages, we have investigated the temperature dependence of the kinetic processes revealed by amperometry recordings of catecholamine release from PC12 cells. This analysis shows that all of the steps related to fusion pore transitions have large activation energies. After the fusion pore has started to expand, subsequent kinetic steps are limited by bulk diffusion. Thus, fusion pore transitions appear to play little, if any, role in exocytosis after the onset of fusion pore dilation.

MATERIALS AND METHODS

Cell Culture

PC12 cells were cultured in 100-mm dishes with Dulbecco's modified Eagle's medium (DMEM) supplemented with 4.5 mg/ml glucose, 3.7 mg/ml $NaHCO_3$, 5% equine serum, and 5% iron-supplemented bovine calf serum at 37°C in a 10% CO_2–air atmosphere (Hay and Martin, 1992). For amperometry recording, cells were transferred to 35-mm plastic culture dishes coated with collagen-I (BD Bioscience) and poly-D-lysine (Sigma-Aldrich). This laboratory has noted previously that this coating of coverslips alters a number of the rates associated with exocytosis from PC12 cells (Han and Jackson, 2006). Cells were preloaded with 1.5 mM norepinephrine and 0.5 mM ascorbate (Sigma-Aldrich) for 16 h before recording (Wang et al., 2001).

Amperometry

Amperometry recording follows methods detailed by Chow and von Rüden (1995) and Wang et al. (2006). Carbon fiber electrodes (ALA Scientific), polarized to 650 mV, were positioned with a micromanipulator to gently touch the surface of a cell. Amperometric current was recorded with a VA-10 amplifier (ALA Scientific), low-pass filtered at 1 kHz, and read into a PC at a digitization rate of 4 kHz using an interface and pCLAMP-8 software (Axon Instrument/Molecular Devices). During recording, cells were bathed in an incubation buffer containing (in mM) 150 NaCl, 4.2 KCl, 1 NaH_2PO_4, 0.7 $MgCl_2$, 2 $CaCl_2$, and 10 HEPES (pH 7.4). Temperature was controlled with a Peltier unit (PTC-10; ALA Scientific) attached to the microscope stage. Exocytosis was induced by depolarization with a solution of the same composition as incubation buffer but with 105 mM KCl and 5 mM NaCl. This depolarization solution was ejected for 6 s with a pulse of pressure (15–20 PSI) from a micropipette (1–2 μm tip) placed ~10 μm from the recorded cell.

Calcium Current

Whole-cell patch clamp was used to record calcium current, using solutions described previously (Han and Jackson, 2006). Voltage was stepped from −80 mV to various test potentials for 200 ms.

Data Analysis

Feet and spikes of single-vesicle release events were analyzed with a computer program described previously (Wang et al., 2006) and modified further for the present studies. Fig. 1 displays a single-vesicle foot→spike sequence, showing the key features and illustrating the parameters determined in this study. Only spikes with peaks >20 pA were used for analysis of feet. This selection is important for obtaining spikes with clearly resolved feet, and also selects release from sites directly under the carbon fiber electrode, for which release kinetics are less temporally broadened by diffusion (Wightman et al., 1995; Haller et al., 1998). It is important to note that peak spike amplitudes measured here show no significant temperature dependence ($P = 0.15$) so that this selection criteria does not introduce a bias that will vary with temperature.

The onset of a foot was determined by the departure of the signal from the baseline by 5×RMS (root-mean-square) noise. To determine the end of the foot, a line was drawn through the spike rising phase from 35 to 60% of the peak. The foot endpoint was taken as the intercept of this line with the baseline. The onset and end of the foot, as determined by these criteria, defined the open-state duration of the fusion pore. The foot area was integrated in this time interval and the integral divided by the open time to yield the average current amplitude for that foot. Feet with durations briefer than 0.75 ms (three times the sampling rate) were rejected as too brief for accurate analysis. Mean foot duration was determined by fitting the distribution of foot lifetimes to an exponential function using the computer program Origin (OriginLab Corporation).

Spike rise time was taken as the time for the spike to rise from 35 to 60% of its peak. The spike decay time cannot be taken from an exponential fit because the falling phase of a spike is generally not

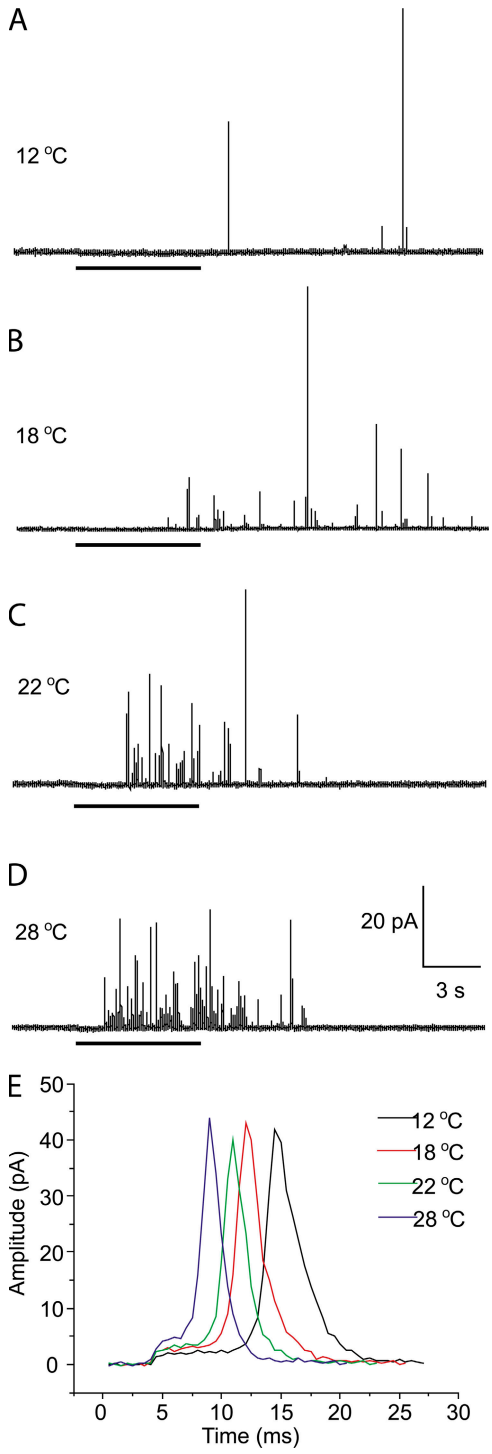

Figure 2. Sample amperometry traces at different temperatures. (A) 12°C. (B) 18°C. (C) 22°C. (D) 28°C. Depolarization by a KCl solution triggered release, and the application time for this solution is indicated by the thick bars below each trace. With this compressed timescale the features illustrated in Fig. 1 are not visible. These traces show the dramatic increase in the frequency of exocytotic events with increasing temperature. Cumulative spike counts pooled from many recordings are plotted in Fig. 3 A. (E) Expanded views of single-vesicle release events were overlaid to show the trends of how prespike feet and spikes change with temperature.

exponential (Schroeder et al., 1992). Instead we measured the time to fall from 90% of peak to within 5×RMS noise of the baseline.

Full-fusion spikes and large kiss-and-run events were analyzed as described previously (Wang et al., 2006). Small kiss-and-run events were also present in our records, and these events can be distinguished on the basis of their small amplitudes (~0.4 pA) and long durations (typically >10 ms) (Wang et al., 2003). These events are considered to reflect a pathway of exocytosis distinct from that which produces full-fusion spikes and these events were not analyzed here because they are more difficult to study in control cells. Large kiss-and-run events with amplitudes close to those of feet are interpreted as transient openings of a fusion pore with the capacity for expansion and full fusion (Wang et al., 2006). These events have roughly rectangular shapes and peak amplitudes between 2 and 3.5 pA. Nonrectangular events larger than 3.5 pA were considered as full fusion events. The number of large kiss-and-run events and full fusion events were counted from the first trace recorded from each cell. These frequencies were then averaged over many cells.

Activation energies (E_a) were determined by linear fitting to Arrhenius plots. The slope yields E_a/R, where R, the gas constant, is 1.98 cal/°K.

RESULTS

Amperometric recordings were made with release triggered by depolarization at temperatures ranging from 12 to 28°C. Fig. 2 shows representative recordings at four selected temperatures. These recordings make it clear that the rate of release increases sharply with temperature, and are consistent with the steep temperature dependence of norepinephrine release from PC12 cells determined by rotating disk voltammetry (Earles et al., 2001).

Peak Ca^{2+} current was measured at 15 and 22°C, yielding values of -71 ± 6 pA ($n = 5$) and -100 ± 22 pA ($n = 7$), respectively. These values are not significantly different. Furthermore, Ca^{2+} channels activate with millisecond kinetics compared with the time scale of seconds for activation of exocytosis. Ca^{2+} current in PC12 cells inactivates only slightly, and the initial lag in exocytosis from PC12 cells also appears in permeable cells (Wang et al., 2003, 2006) where the gating of Ca^{2+} channels is irrelevant. Thus, in contrast to synapses, where the activation of Ca^{2+} channels plays an important role in release kinetics (Sabatini and Regehr, 1996), exocytosis in PC12 cells is too slow to reflect Ca^{2+} activation. For these reasons, the temperature dependence of Ca^{2+} influx was not considered further. To determine how the individual rate processes contribute to the temperature dependence of exocytosis, we conducted a detailed analysis of both spikes and feet.

Spike Frequency

To quantify the temperature-dependent increase in exocytosis illustrated in Fig. 2, we compiled counts of numbers of spikes at different time points for 27 or more cells at each temperature. Cumulative spike counts were then plotted versus time for each temperature (Fig. 3 A). These plots show a characteristic initial lag before secretion becomes vigorous and we have previously decomposed

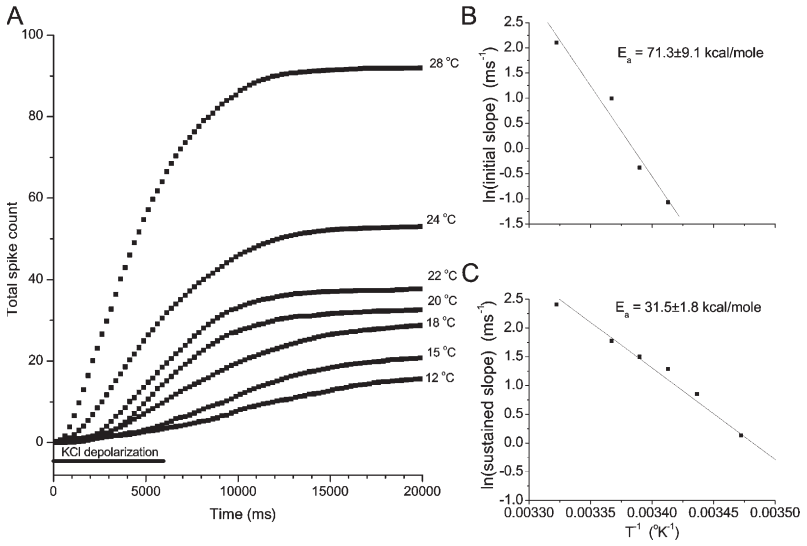

Figure 3. The temperature dependence of cumulative spike plots. (A) Spikes were counted from traces such as those displayed in Fig. 2. Traces from 27 or more cells at each temperature were combined and normalized to the number of recordings. In each plot a point at a given time is the total number of spikes (>2 pA), seen up to that time point, per recording. The bar below the plot indicates the 6 s during which the cells were depolarized by pressure application of a high KCl solution. (B) The initial slope in the first 2 s was measured for each temperature. The logarithms of these slopes were then plotted versus one over the absolute temperature to give an Arrhenius plot. The activation energy, E_a, was obtained from the slope of this plot. (C) The sustained slopes of the cumulative spike plots in A were taken as the slope of the segment between 2 and 7 s. An Arrhenius plot was constructed as in B.

such plots into initial and sustained frequencies of fusion events corresponding to the slope seen in the first 2 s and the slope 2–7 s after the onset of KCl depolarization, respectively (Han and Jackson, 2006). These two slopes are taken as reflections of distinct early and late kinetic steps in exocytosis that precede fusion pore opening. Because the fusion event frequency is maximal in the 2–7-s time window the sustained velocity is also the maximal velocity of vesicle fusion events. The Arrhenius plots of these frequencies in Fig. 3 (B and C) show that both processes have large activation energies. (Secretion was so slow at the lowest temperatures that we could not determine initial slopes so the plot of initial slope has fewer points.) For the initial slope, the Arrhenius plot yielded E_a = 71.3 kcal/mole and for the sustained slope we obtained 31.5 kcal/mole. Table I presents all of the activation energies measured in the present study.

Spike Dimensions

In contrast to parameters related to the frequency of spike events (Fig. 3), parameters related to the dimensions and shape of individual spikes depend weakly on temperature. Spikes rise and decay more rapidly with increasing temperature, with width at half-height decreasing from 2.00 ± 0.05 ms at 12°C to 1.46 ± 0.03 ms at 28°C. Note that these spike widths are for spikes with peak amplitudes >20 pA. If the average includes spikes with peaks between 5 and 20 pA, then the width increases by ~75%. We determined rise and decay times from spikes as indicated in Materials and methods (Fig. 1) and displayed the temperature dependence of these quantities in Arrhenius plots (Fig. 4; note that the abscissa is the logarithm of the inverse of the rise or decay time). The activation energies from these plots are much lower than those for spike frequency, and Table I presents these values for comparison.

The peak amplitude and area of spikes changed very little as temperature varied (Fig. 5, A and B). The temperature dependences of these quantities are presented as standard plots rather than as Arrhenius plots because they have no simple relation to rate processes. Mean spike amplitude showed no statistically significant dependence on temperature (P = 0.15). Integrated spike area decreased from 111 to 85 fC over the temperature range studied, and this weak temperature dependence was statistically significant (P = 0.004). The activation energies for spike frequency and shape parameters are presented in Table I.

The fraction of total events that are large kiss-and-run events was determined as described in Materials and methods. This quantity shows a clear and statistically significant decrease with increasing temperature (Fig. 5 C; P = 0.012). This plot indicates that lower temperatures increase the relative probability of kiss-and-run versus full fusion by ~50%.

Fusion Pore Amplitude and Kinetics

Arrhenius plots of foot amplitude show a weak increase with temperature and relatively small activation energy (Fig. 6 A; E_a = 6.2 kcal/mole). These results suggest that

TABLE I

Activation Energies

Spike parameters				Foot parameters		
Initial frequency	Sustained frequency	Rise time	Decay time	Amplitude	k_c	k_d
71.3 ± 9.1	31.5 ± 1.8	2.1 ± 0.4	4.3 ± 1.2	6.2 ± 0.7	10.0 ± 0.7	17.3 ± 1.5

Activation energies determined from linear fits to Arrhenius plots (see Figs. 3–5). Units kcal/mole.

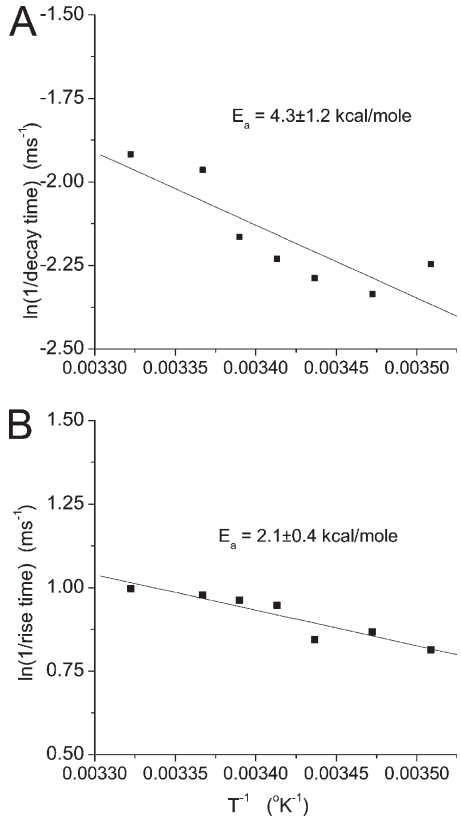

Figure 4. The temperature dependence of spike rise and decay times. Rise and decay times of a spike are indicated in Fig. 1. These values were determined for many spikes (386–1981) at each temperature, plotted, and fitted to a line to yield the activation energies.

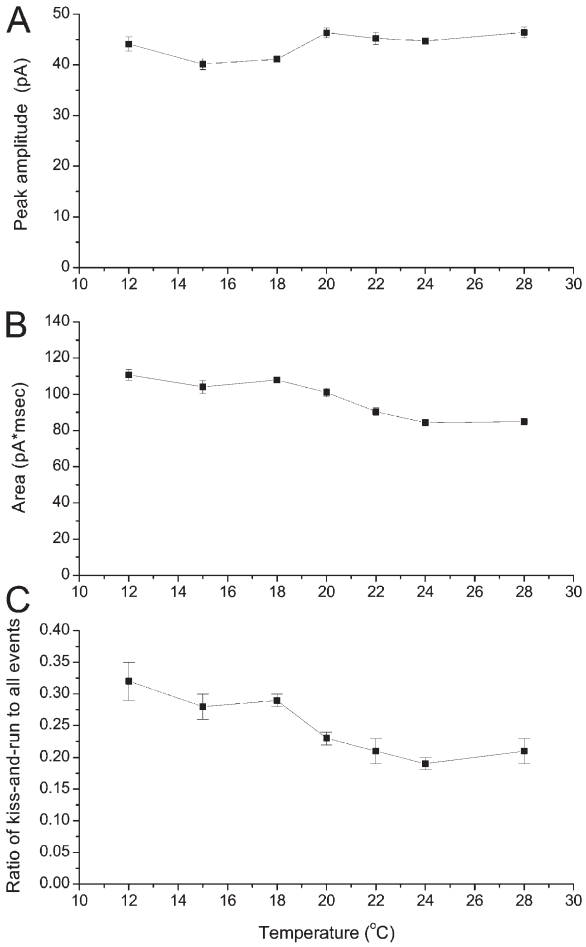

Figure 5. Plots of peak spike amplitude (A), spike area (B), and kiss-and-run fraction (C) versus temperature. Peak amplitude showed no temperature dependence but area and fraction did (see text).

flux through the open fusion pore does not entail crossing a large energy barrier. By contrast the mean open-state duration of a fusion pore decreases more strongly with temperature, and an Arrhenius plot of the inverse of this quantity yields a larger activation energy (Fig. 6 B; E_a = 15.4 kcal/mole).

Fusion pores can terminate by either closing or dilating (see scheme at the top of Fig. 6). The rate constants for these two processes, k_c and k_d, respectively, can be determined with the aid of a model for fusion pore kinetics incorporating these two transitions (Wang et al., 2006). This model leads to expressions for the open-state duration and fraction of large kiss-and-run events in terms of the closing rate constant, k_c, and the dilating rate constant, k_d (Eqs. 1 and 3 of Wang et al., 2006). With experimentally determined values for this fraction (Fig. 5 C) and the fusion pore mean open time (Fig. 6 B) we solved for k_c and k_d at each temperature to obtain values plotted in Fig. 6 (C and D). For k_c we obtained E_a = 10.0 kcal/mole and for k_d we obtained 17.3 kcal/mole (Table I).

DISCUSSION

This study has reported the results of an investigation of the temperature dependence of exocytosis, providing a detailed kinetic analysis of several distinct steps and processes that can be resolved in amperometry recordings. Although temperature is a very blunt probe of mechanism, this analysis may be useful as a basic framework for evaluating temperature effects on synapses. In particular, we saw that kiss-and-run becomes significantly more common at lower temperatures and this observation may be useful in studies of this elusive form of release at synapses.

The present results offer some interesting perspectives on some important mechanistic questions. The rate processes underlying the various steps of exocytosis vary considerably in their dependence on temperature, and can be divided into two basic categories on the basis of qualitative behavior. The activation energies in Table I illustrate this trend. The foot amplitude, spike rise time, and spike decay time have E_a values ranging from 2.1 to 6.2 kcal/mole. These processes thus have temperature dependences similar to those seen for bulk diffusion, which in the case of ions follows the temperature dependence of water viscosity (Robinson and Stokes, 1965). By contrast, the fusion pore rate constants, k_d and k_c,

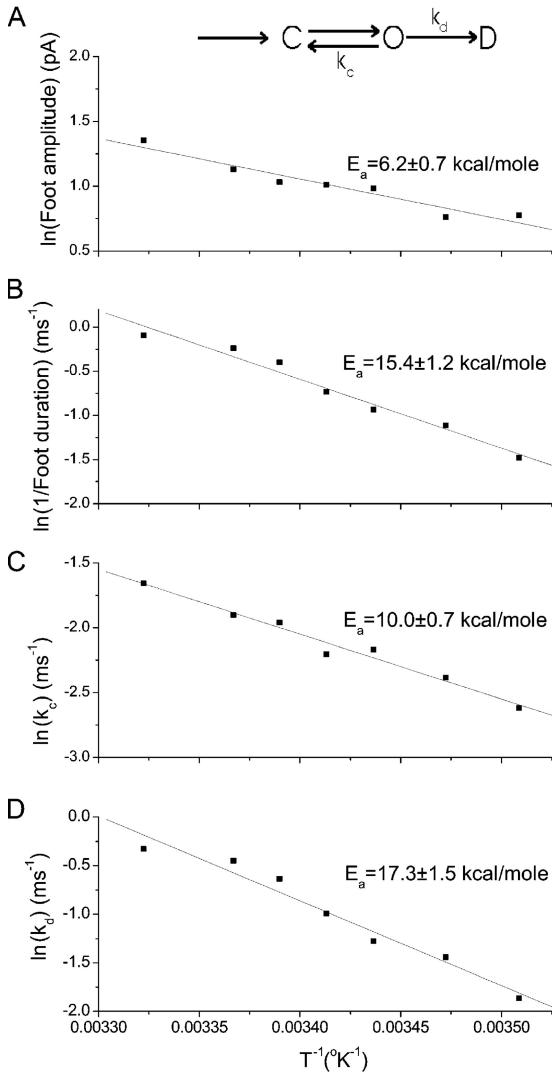

Figure 6. Temperature dependence of fusion pores. The kinetic scheme at the top indicates the formation of a closed fusion pore, C, and the transition to the open state, O. The open state can close with rate k_c or enter the dilating phase, D, with rate k_d. Arrhenius plots are presented for (A) foot amplitude, (B) 1/(mean foot duration), (C) k_c, and (D) k_d. k_c and k_d were determined from the mean lifetime (Fig. 6 B) and fraction of large kiss-and-run events (Fig. 5 C) as described in the text and in Wang et al. (2006).

as well as the spike frequencies depend more strongly on temperature, and this implies a nondiffusive process, possibly one involving structural rearrangements of the lipids and proteins of the fusing membranes.

The foot amplitude reflects the rate with which norepinephrine permeates the initial fusion pore. This structure is generally hypothesized to have a diameter on the order of 1 nm and a length on the order of 10 nm to permit the spanning of two lipid bilayers (Spruce et al., 1990; Lindau and Almers, 1995; Klyachko and Jackson, 2002; Han et al., 2004). This long narrow pathway thus has dimensions similar to an ion channel, and one can use the advances in understanding ion permeation in ion channels as a guide in the interpretation of the permeation rate for norepinephrine in a fusion pore.

It has long been recognized that an aqueous pore through a lipid membrane should present a large energy barrier due to the image force between an ion and the weakly polarizable hydrocarbon membrane interior (Parsegian, 1969; Kuyucak et al., 2001). Norepinephrine should have a positive charge at neutral pH, and the effects of charge mutations in the syntaxin membrane anchor indicate that the charged species permeates fusion pores (Han and Jackson, 2005). However, the activation energy for pore flux is much lower than typical estimates based on image force calculations. In fact, this paradox recapitulates the trend noted for ion permeation of ion channels, where the barriers inferred from experiment are generally much lower than can be explained by energetic calculations (Jackson, 1984; Kuyucak et al., 2001). Thus, as with ion channels, fusion pores present lower than expected energy barriers for the permeation of charged species, and the reasons for this are not well understood.

The initial slope of the cumulative spike plot (Fig. 3 B) had the largest E_a value (Table I). This is the earliest kinetic step that we can see, and it is thus of interest that what may be the entry step has the highest energy barrier. The large E_a values for the initial and sustained spike frequency as well as for the fusion pore dilation rate suggest that these are the processes responsible for the strong temperature dependence of Ca^{2+}-triggered exocytosis in PC12 cells (Earles et al., 2001) and possibly in synapses as well (Takeuchi, 1958; Katz and Miledi, 1965; Weight and Erulkar, 1976; Sabatini and Regehr, 1996; Volgushev et al., 2004). Furthermore, these large E_a values suggest that these transitions require significant structural rearrangements.

The structural intermediates hypothesized to play a role in lipid fusion have large energies in the range encompassing the energies observed here (Chernomordik and Kozlov, 2003). Activation energies for conformational transitions in proteins are also generally large (Johnson et al., 1954), so our results do not offer evidence in favor of lipidic versus proteinaceous fusion pores. The fusion pore closing rate in mast cells undergoes an abrupt transition at 13°C, and this discontinuity suggests that the fluidity of the lipids plays a permissive role in the pore closing transition (Oberhauser et al., 1992). We saw no such break in any of our plots but we only went down to 12°C so we cannot rule out the possibility of an abrupt transition at a lower temperature. In mast cells at temperatures above the transition, the E_a for fusion pore closure of 7 kcal/mole is not very different from the value of 10 kcal/mole reported here in PC12 cells. The activation energy for synaptotagmin I binding to phospholipids is relatively low (3.2 kcal/mole for rat synaptotagmin I binding to PS/PC liposomes) (Hui et al., 2005), but that is a second order process that is probably

diffusion limited. Synaptotagmin I release from liposomes upon removal of Ca^{2+} has a higher activation energy (7.2 kcal/mole; Hui et al., 2005), but this process is less relevant to the Ca^{2+}-initiated process we are investigating.

The quantities characterizing the shape of a spike depend only weakly on temperature. These include the peak amplitude, total area, rise time, and decay time. The weak temperature dependences of amplitude and area are in line with the weak temperature dependences of the total charge of miniature synaptic currents (Cohen and Van der Kloot, 1983; Kushmerick et al., 2006). If the shape and dimensions of a spike were influenced by fusion pore transitions we would expect a steeper temperature dependence. Instead, our results indicate that the shape of a spike is governed by diffusion from the site of release to the carbon fiber electrode, rather than by fusion pore transitions. Detailed analysis of spike shape with the aid of diffusion models has suggested that spikes recorded by an electrode positioned within 1 μm from the cell surface are roughly three times broader than the predictions of a diffusion model (Wightman et al., 1995; Haller et al., 1998). These results were interpreted to indicate that release in the final stage of fusion is limited by dissociation of catecholamine from the protein matrix of a dense-core vesicle. However, our spikes are less than half as broad as spikes recorded from PC12 cells by another laboratory (Colliver et al., 2000). This could reflect a subtle difference in our conditions that weakens the interaction with the vesicle matrix. Our spike duration is close to that predicted for diffusion from a site directly under the recording electrode (Wightman et al., 1995; Haller et al., 1998). Furthermore, broadening a spike by threefold may not require very strong binding. To slow a kinetic process by a factor of three requires a binding energy that is only slightly larger than RT, and we obtained an E_a for spike decay time of 4.3 kcal/mole, which is already approximately seven times greater than RT. When one considers the question of whether matrix dissociation or diffusion through a fusion pore limits the rate of catecholamine efflux, if both factors have comparable weights then small changes or variations in matrix properties and fusion pore dimensions could shift the balance and allow different factors to become rate limiting. Thus, matrix dissociation may be limiting under some conditions, but small changes in experimental conditions or the condition of cells could allow diffusion to become limiting.

Regardless of whether spike shape is determined by diffusion or matrix dissociation, neither of these mechanisms depends on fusion pore transitions, and this leaves an interesting problem unsolved. Molecular manipulations of MUNC18 (Fisher et al., 2001), cysteine string protein (Graham and Burgoyne, 2000), and complexin II (Archer et al., 2002) have been reported to alter the shapes of spikes. We have found similar effects with synaptotagmin isoforms and mutants (Wang, 2001; Wang et al., 2001) along with the SNARE proteins, synaptobrevin, SNAP-25, and syntaxin (Han, X., personal communication; unpublished data). In contrast to changes in prespike foot duration, which can be attributed to a change in the stability of an initial fusion pore (Wang, 2001), the rise and decay times of amperometric spikes appear not to depend on structural intermediates in the fusion apparatus. If the speed of spike rise reflects the rate of fusion pore expansion, we should see a stronger temperature dependence of the rise time (Fig. 4 B). If fusion pores can expand and then reseal before content expulsion was complete, we should see stronger temperature dependences of area (Fig. 5 A). However, if spike shape parameters are determined by diffusion, we are left with the mystery of explaining how proteins in the vesicle and plasma membranes could alter the bulk diffusion of norepinephrine. If the affinity of the vesicular matrix for norepinephrine contributes to spike shape kinetics (Wightman et al., 1995; Haller et al., 1998), then it might be possible for expression of different proteins to alter the expression of vesicle matrix proteins. This might explain the effects of molecular manipulations on spike shape. Despite its weak temperature dependence, the spike shape does in some way depend on the molecules that form the fusion apparatus. It is hoped that future investigations will explain how.

We thank Edwin Chapman, Zhenjie Zhang, and Enfu Hui for discussions and comments on this manuscript.

This work was supported by National Institutes of Health grant NS44057.

David C. Gadsby served as editor.

Submitted: 21 September 2007
Accepted: 13 December 2007

REFERENCES

Ales, E., L. Tabares, J.M. Poyato, V. Valero, M. Lindau, and G. Alvarez de Toledo. 1999. High calcium concentrations shift the mode of exocytosis to the kiss-and-run mechanism. *Nat. Cell Biol.* 1:40–44.

Archer, D.A., M.E. Graham, and R.D. Burgoyne. 2002. Complexin regulates the closure of the fusion pore during regulated vesicle exocytosis. *J. Biol. Chem.* 277:18249–18252.

Chernomordik, L.V., and M.M. Kozlov. 2003. Protein-lipid interplay in fusion and fission of biological membranes. *Annu. Rev. Biochem.* 72:175–207.

Chow, R.H., and L. von Rüden. 1995. Electrochemical detection of secretion from single cells. *In* Single-Channel Recording. B. Sakmann and E. Neher, editors. Plenum Press, New York. 245–275.

Chow, R.H., L. von Rüden, and E. Neher. 1992. Delay in vesicle fusion revealed by electrochemical monitoring of single secretory events in adrenal chromaffin cells. *Nature.* 356:60–63.

Cohen, I.S., and W. Van der Kloot. 1983. Effects of low temperature and terminal membrane potential on quantal size at frog neuromuscular junction. *J. Physiol.* 336:335–344.

Colliver, T.L., E.J. Hess, E.N. Pothos, D. Sulzer, and A.G. Ewing. 2000. Quantitative and statistical analysis of the shape of amperometric spikes recorded from two populations of cells. *J. Neurochem.* 74:1086–1097.

Earles, C.A., J. Bai, P. Wang, and E.R. Chapman. 2001. The tandem C2 domains of synaptotagmin contain redundant Ca^{2+} binding sites that cooperate to engage t-SNAREs and trigger exocytosis. *J. Cell Biol.* 154:1117–1123.

Fisher, R.J., J. Pevsner, and R.D. Burgoyne. 2001. Control of fusion pore dynamics during exocytosis by Munc18. *Science.* 291:875–878.

Graham, M.E., and R.D. Burgoyne. 2000. Comparison of cysteine string protein (Csp) and mutant α-SNAP overexpression reveals a role for csp in late steps of membrane fusion in dense-core granule exocytosis in adrenal chromaffin cells. *J. Neurosci.* 20:1281–1289.

Haller, M., C. Heinemann, R.H. Chow, R. Heidelberger, and E. Neher. 1998. Comparison of secretory responses as measured by membrane capacitance and by amperometry. *Biophys. J.* 74:2100–2113.

Han, X., and M.B. Jackson. 2005. Electrostatic interactions between the syntaxin membrane anchor and neurotransmitter passing through the fusion pore. *Biophys. J.* 88:L20–L22.

Han, X., and M.B. Jackson. 2006. Structural transitions in the synaptic SNARE complex during Ca^{2+}-triggered exocytosis. *J. Cell Biol.* 172:281–293.

Han, X., C.T. Wang, J. Bai, E.R. Chapman, and M.B. Jackson. 2004. Transmembrane segments of syntaxin line the fusion pore of Ca^{2+}-triggered exocytosis. *Science.* 304:289–292.

Hay, J.C., and T.F.J. Martin. 1992. Resolution of regulated secretion into sequential MgATP-dependent and calcium-dependent stages mediated by distinct cytosolic proteins. *J. Cell Biol.* 119:139–151.

Hui, E., J. Bai, P. Wang, M. Sugimori, R.R. Llinas, and E.R. Chapman. 2005. Three distinct kinetic groupings of the synaptotagmin family: candidate sensors for rapid and delayed exocytosis. *Proc. Natl. Acad. Sci. USA.* 102:5210–5214.

Jackson, M.B. 1984. The electrostatic activation enthalpy for ion transport through a membrane channel. *Biophys. J.* 45:99–100.

Jackson, M.B. 2007. In search of the fusion pore of exocytosis. *Biophys. Chem.* 126:201–208.

Jankowski, J.A., T.J. Schroeder, E.L. Ciolkowski, and R.M. Wightman. 1993. Temporal characteristics of quantal secretion of catecholamines from adrenal medullary cells. *J. Biol. Chem.* 268:14694–14700.

Johnson, F.H., H. Eyring, and M.J. Polissar. 1954. Ch. 8. Temperature. *In* The Kinetics of Molecular Biology. John Wiley & Sons, New York. 187–285.

Katz, B., and R. Miledi. 1965. The effect of temperature on the synaptic delay at the neuromuscular junction. *J. Physiol.* 181:656–670.

Klyachko, V.A., and M.B. Jackson. 2002. Capacitance steps and fusion pores of small and large-dense-core vesicles in nerve terminals. *Nature.* 418:89–92.

Kushmerick, C., R. Renden, and H. von Gersdorff. 2006. Physiological temperatures reduce the rate of vesicle pool depletion and short-term depression via an acceleration of vesicle recruitment. *J. Neurosci.* 26:1366–1377.

Kuyucak, S., O.S. Andersen, and S.-H. Chung. 2001. Models of permeation in ion channels. *Rep. Prog. Phys.* 64:1427–1472.

Lindau, M., and W. Almers. 1995. Structure and function of fusion pores in exocytosis and ectoplasmic membrane fusion. *Curr. Opin. Cell Biol.* 7:509–517.

Oberhauser, A.F., J.R. Monck, and J.M. Fernandez. 1992. Events leading to the opening and closing of the exocytotic fusion pore have markedly different temperature dependencies. Kinetic analysis of single fusion events in patch-clamped mouse mast cells. *Biophys. J.* 61:800–809.

Parsegian, A. 1969. Energy of an ion crossing a low dielectric membrane: solutions to four relevant electrostatic problems. *Nature.* 221:844–846.

Robinson, R.A., and G. Stokes. 1965. Electrolyte Solutions. Butterworth & Co., London. 571 pp.

Sabatini, B.L., and W.G. Regehr. 1996. Timing of neurotransmission at fast synapses in the mammalian brain. *Nature.* 384:170–172.

Schroeder, T.J., J.A. Jankowski, K.T. Kawagoe, R.M. Wightman, C. Lefrou, and C. Amatore. 1992. Analysis of diffusional broadening of vesicular packets of catecholamines released from biological cells during exocytosis. *Anal. Chem.* 64:3077–3083.

Spruce, A.E., L.J. Breckenridge, A.K. Lee, and W. Almers. 1990. Properties of the fusion pore that forms during exocytosis of a mast cell secretory vesicle. *Neuron.* 4:643–654.

Takeuchi, N. 1958. The effect of temperature on the neuromuscular junction of the frog. *Jpn. J. Physiol.* 8:391–404.

Volgushev, M., I. Kudryashov, M. Chistiakova, M. Mukovski, J. Niesmann, and U.T. Eysel. 2004. Probability of transmitter release at neocortical synapses at different temperatures. *J. Neurophysiol.* 92:212–220.

Wang, C.T. 2001. Kinetics and molecular mechanisms of calcium-regulated exocytosis of catecholamines. Ph.D., University of Wisconsin, Madison. 135 pp.

Wang, C.T., R. Grishanin, C.A. Earles, P.Y. Chang, T.F. Martin, E.R. Chapman, and M.B. Jackson. 2001. Synaptotagmin modulation of fusion pore kinetics in regulated exocytosis of dense-core vesicles. *Science.* 294:1111–1115.

Wang, C.T., J.C. Lu, J. Bai, P.Y. Chang, T.F. Martin, E.R. Chapman, and M.B. Jackson. 2003. Different domains of synaptotagmin control the choice between kiss-and-run and full fusion. *Nature.* 424:943–947.

Wang, C.T., J. Bai, P.Y. Chang, E.R. Chapman, and M.B. Jackson. 2006. Synaptotagmin-Ca2+ triggers two sequential steps in regulated exocytosis in rat PC12 cells: fusion pore opening and fusion pore dilation. *J. Physiol.* 570:295–307.

Weight, F.F., and S.D. Erulkar. 1976. Synaptic transmission and effects of temperature at the squid giant synapse. *Nature.* 261:720–722.

Wightman, R.M., J.A. Jankowski, R.T. Kennedy, K.T. Kawagoe, T.J. Schroeder, D.J. Leszczyszyn, J.A. Near, E.J. Diliberto Jr., and O.H. Viveros. 1991. Temporally resolved catecholamine spikes correspond to single vesicle release from individual chromaffin cells. *Proc. Natl. Acad. Sci. USA.* 88:10754–10758.

Wightman, R.M., T.J. Schroeder, J.M. Finnegan, E.L. Ciolkowski, and K. Pihel. 1995. Time course of release of catecholamines from individual vesicles during exocytosis at adrenal medullary cells. *Biophys. J.* 68:383–390.

Zhou, Z., S. Misler, and R.H. Chow. 1996. Rapid fluctuations in transmitter release from single vesicles in bovine adrenal chromaffin cells. *Biophys. J.* 70:1543–1552.